

A Mathematical Analysis for Spark Ignition for Premixed Flame Based on Extended Perfectly Stirred Reactor (PSR) Model

Felipe C. Minuzzi¹

Department of Mathematics, UFSM, Santa Maria, RS, Brazil

Chunkan Yu²

Institute of Technical Thermodynamics, KIT, Karlsruhe, Germany

Abstract. This study improves the traditional Perfectly Stirred Reactor (PSR) model by incorporating an additional energy source to more accurately represent the spark ignition process in a laminar premixed flame within a counterflow configuration. A non-dimensional system of governing ordinary differential equations (ODEs) is formulated to describe the behavior of temperature and fuel concentration under these conditions. A mathematical analysis is conducted to assess the stability of steady-state solutions in the dynamic system, utilizing the large activation energy asymptotic limit as a primary analytical tool. Analytical solutions for stable regimes, characterized by negative eigenvalues, are derived and it is found that the equilibrium steady states exhibit two stable regimes: one corresponding to failed ignition and the other to successful ignition.

Keywords. PSR, spark ignition, dynamic system, reactive flows

1 Introduction

Combustion efficiency can be optimized through a better understanding of the spark ignition process of premixed combustible gas mixtures. In [4], numerical investigation has been performed to understand the effect of the initial pressure wave generated by the spark on the minimum ignition energy (MIE), which is a fundamental parameter to determine the success or failure of ignition process in different operational conditions. The study highlights the importance of accounting for pressure wave dynamics in accurately predicting MIE in practical combustion systems. Further investigations such as [8, 9] calculate MIE for a range of parameters, including mixture compositions, pressures, radii of external energy sources, and ignition times. These studies offer valuable insights into how these factors affect the energy threshold needed to ignite premixed gases, providing crucial information for both cylindrical and spherical geometries.

Recently, the relatively new configuration of spark ignition of laminar premixed flame in counterflow [11, 12] has been proposed and numerically investigated. This configuration enables the examination of the spark ignition process under a constant flame strain rate, a parameter that characterizes both the flow velocity and the velocity gradient along the flame surface. This approach significantly simplifies the complexities encountered in spherical flames, where the flame strain rate undergoes instantaneous changes during flame propagation [3, 5].

In [11, 12], it was reported that the MIE increases with larger flow velocity, as more gas mixture passes through the energy source region. Additionally, at short spark duration times, the MIE

¹felipe.minuzzi@ufsm.br

²chunkan.yu@kit.edu

shows only minor changes. Thus, one might ask if these conclusions can be extended to another gas mixture since, although this configuration has been investigated for both methane/hydrogen/air and ammonia/hydrogen/air mixtures, there is no simple theoretical formulation discussing the effect of flow conditions on the spark ignition process for this configuration.

In order to answer this question, the spark ignition process in a laminar strained premixed flame is modeled by means of the classic Perfectly Stirred Reactor (PSR) by introducing an additional energy source. The corresponding residence time describes the rate of mass transport, which can be used to directly compare with the chemical reaction rate.

2 Mathematical Modeling

In the present work, the classic Perfectly Stirred Reactor (PSR) model [10] is selected, and an external spark energy source is considered, which provides energy to the gas mixture inside the PSR. In this PSR model, temperature and species concentrations are spatially homogeneously distributed within the system. Initially, the reactor is filled with an unburnt premixed gas mixture, which is heated by the spark ignition energy. Throughout the process, fresh unburnt gas, corresponding to the initial state of the gas inside the PSR, enters the reactor, mixes with the heated gas mixture, cools it down, and subsequently exits the reactor. To determine whether the spark ignition process is successful, we can simply examine the steady state of the PSR model. If the gas mixture leaves the reactor with the same thermo-kinetic properties as the fresh unburnt gas mixture, then ignition has not been successful. However, if the exiting gas mixture exhibits a high temperature and consists of combustion products, ignition can be considered successful. Unlike the conventional PSR model, when additional ignition energy is introduced, we are not limited to analyzing only the steady-state behavior. Instead, we can also investigate the entire ignition process, including the transient evolution leading up to the steady state.

When considering the PSR model, we take into account not only the chemical reaction rate but also the residence time, a physical timescale that describes the mixing process. Therefore, this model can be used to further investigate the impact of different physical timescales on the chemical reaction process.

To simplify the analysis, we consider an adiabatic condition, in which no heat loss from the reactor to the surroundings occurs. This is a reasonable simplification since the entire chemical process takes place rapidly. Furthermore, all physical properties such as $\tilde{\rho}$ and isobaric heat capacity \tilde{c}_p are regarded as constant values. For the chemistry, a one-step global reaction $F(\text{uel}) \rightarrow P(\text{product})$ is applied and the reaction rate is governed by the Arrhenius law with first reaction order.

Based on these assumptions, the following conservation equations for energy in terms of temperature \tilde{T} inside the reactor and volumetric fuel concentration \tilde{c}_F can be written as:

$$\tilde{\rho} \tilde{c}_p \frac{d\tilde{T}}{d\tilde{t}} = -\tilde{\rho} \tilde{c}_p \frac{\tilde{T} - \tilde{T}_{\text{in}}}{\tilde{\tau}_R} + \tilde{Q} \dot{\tilde{\omega}}_F + \dot{\tilde{E}}_s \quad (1)$$

$$\frac{d\tilde{c}_F}{d\tilde{t}} = -\frac{\tilde{c}_F - \tilde{c}_{F,\text{in}}}{\tilde{\tau}_R} - \dot{\tilde{\omega}}_F. \quad (2)$$

In both equations, $\tilde{\tau}_R$ is the residence time, a physical timescale describing the mixing process between mixture inside the reactor and fresh unburnt gas entering the reactor. The thermo-kinetic states of the incoming fresh gas mixture entering the reactor are described by the temperature \tilde{T}_{in} and volumetric fuel concentration $\tilde{c}_{F,\text{in}}$. \tilde{Q} denotes the heat release of the chemical reaction, and $\dot{\tilde{\omega}}_F$ the consumption rate of fuel due to chemical reaction, which is expressed as:

$$\dot{\tilde{\omega}}_F = \tilde{A} \tilde{c}_F \exp\left(-\frac{\tilde{E}_a}{R \tilde{T}}\right), \quad (3)$$

where \tilde{A} is the pre-exponential factor, \tilde{E}_a the activation energy and \tilde{R} the universal gas constant.

For power of spark ignition energy $\dot{\tilde{E}}_s$, it follows the case conditions that i) $\dot{\tilde{E}}_s = \tilde{E}_s/\tilde{\tau}_s$ for $\tilde{t} \leq \tilde{\tau}_s$; and ii) $\dot{\tilde{E}}_s = 0$ for $\tilde{t} > \tilde{\tau}_s$, in which $\tilde{\tau}_s$ is the spark deposited time, and \tilde{E}_s the volumetric total spark ignition energy.

In order to simplify the analysis, we introduce several dimensionless variables: dimensionless activation energy β , dimensionless heat release B , dimensionless time t , dimensionless fuel concentration c_F , dimensionless temperature θ and Damköhler number Da , which are defined as

$$\begin{aligned}\beta &= \frac{\tilde{E}_a}{\tilde{R}\tilde{T}_{\text{in}}}, & B &= \frac{\tilde{Q}\beta}{\tilde{\rho}\tilde{c}_p\tilde{T}_{\text{in}}}\tilde{c}_{F,\text{in}}, & t &= \frac{\tilde{t}}{\tilde{\tau}_R}, & c_F &= \frac{\tilde{c}_{F,\text{in}} - \tilde{c}_F}{\tilde{c}_{F,\text{in}}}, \\ \theta &= \frac{\beta(\tilde{T} - \tilde{T}_{\text{in}})}{\tilde{T}_{\text{in}}}, & Da &= \frac{\tau_R}{\tau_{\text{chem}}} = \frac{\tilde{\tau}_R}{[\tilde{A} \exp(-\beta)]^{-1}}.\end{aligned}\quad (4)$$

For $c_F = 0$, the gas mixture consists only of fuel, while for $c_F = 1$, the fuel is fully converted into product. For $0 < c_F < 1$, the gas mixture consists of both fuel and product.

Among these dimensionless variables, the dimensionless activation energy β , the dimensionless heat release B , and the Damköhler number Da are three most important quantities which are used to describe the chemical reaction (β and B) and the coupling between chemistry and physical process (Da). The dimensionless activation energy β is typically considered to be in the range of $30 \leq \beta \leq 50$ for a combustion system [2, 13]. The dimensionless heat release B can have a wide value range: B with small value indicates a weak exothermic chemical reaction; while B with a large value represents a strong exothermic chemical reaction. The third dimensionless parameter, the Damköhler number (Da), plays a key role in characterizing the ratio between the flow timescale (specifically, the residence time) and the chemical reaction time scale. When $Da \rightarrow \infty$, it indicates that the chemical reaction proceeds infinitely fast.

By applying these dimensionless variables, the above-mentioned governing equation can be rewritten in dimensionless form as

$$\frac{d\theta}{dt} = -\theta + BDa(1 - c_F) \exp\left(\frac{\theta}{1 + \theta/\beta}\right) + \dot{e}_s, \quad \text{with } \dot{e}_s = \begin{cases} \frac{e_s}{\tau_s} & (t \leq \tau_s) \\ 0 & (t > \tau_s) \end{cases} \quad (5)$$

$$\frac{dc_F}{dt} = -c_F + Da(1 - c_F) \exp\left(\frac{\theta}{1 + \theta/\beta}\right), \quad (6)$$

with the initial condition

$$\theta(t = 0) = 0, \quad \text{and} \quad c_F(t = 0) = 0. \quad (7)$$

At steady state, if the mixture leaves the reactor with $c_F \approx 0$, the system has not been successfully ignited. If the mixture leaves the reactor with $c_F \approx 1$, then most of the fuel has been converted into product, indicating successful ignition.

Figure 1 shows the typical time evolution of dimensionless temperature and fuel concentration for both failed ignition (left) and successful ignition (right). In both cases, the spark duration time is set to 0.1, as indicated by the vertical dashed lines. The key difference between the two scenarios is the amount of spark ignition energy supplied (different values of e_s).

- For a failed ignition, where the spark ignition energy is relatively low (here, $e_s = 0.5$), the dimensionless fuel concentration at steady state drops to approximately 0.01. This indicates that almost no fuel is converted into combustion products, suggesting that the spark energy was insufficient to support the reaction. Consequently, the dimensionless temperature remains well below 1.

- for a successful ignition with sufficiently high spark ignition energy (here, $e_s = 3$), the system behaves very differently. A sharp rise in both temperature and fuel concentration can be observed during ignition. The fuel concentration reaches a steady-state value close to 1.0, suggesting that a significant portion of the fuel undergoes combustion, leading to a substantial temperature increase. The corresponding dimensionless temperature rises to approximately 8.

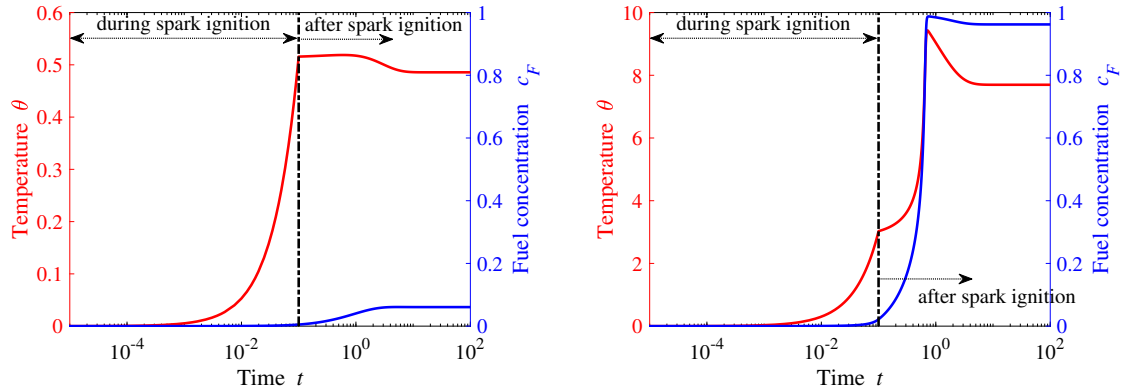


Figure 1: Time-development of dimensionless temperature and fuel concentration for a failed ignition (left, $e_s = 0.5$) and a successful ignition (right, $e_s = 3$). Model parameter: $B = 8$, $\tau_s = 0.1$, $\beta = 40$, $Da^{-1} = 25$. Source: from the authors.

From this example, we observe that, for the same values of dimensionless variables, the dynamic system can evolve toward different steady states depending on the supplied spark ignition energy. This shows that the system is very sensitive to input spark ignition energy. Even a small variation in the spark ignition energy can result in completely different ignition scenarios — either a failed ignition or a successful combustion process.

To get deeper understanding on the mechanisms driving these two totally different scenarios, the following sections will present a mathematical analysis of the dynamic system. This analysis will help evaluate the key factors influencing ignition success and provide a clear understanding of the system's response to varying spark ignition energy.

3 Mathematical Analysis

Now, we investigate some fundamental aspects of the dynamic system, including the stability of the steady-state solutions and how these steady states change with respect to the dimensionless variables. For the steady-state (SS) condition ($d\theta/dt = 0$, $dc_F/dt = 0$), the manifold for the steady-state solution is obtained as:

$$\theta^{ss} = B \cdot c_F^{ss}. \quad (8)$$

It can be observed that the steady-state solution is a linear function with a constant slope, where the slope is determined by the dimensionless heat release variable B . This indicates that the steady-state solution depends solely on the value of B .

Based on the assumption that $\beta \gg 1$ [2, 13], the exponential term can be approximated as $\exp\left(\frac{\theta}{1+\theta/\beta}\right) \approx \exp(\theta)$. Consequently, the Jacobian matrix of the approximated source term from

Eq.(6), together with the steady state solution Eq.(8), can be written as:

$$J(\theta^{ss}) = \begin{pmatrix} -1 + B \, Da \, (1 - \frac{\theta^{ss}}{B}) e^{\theta^{ss}} & -B \, Da \, e^{\theta^{ss}} \\ Da \, (1 - \frac{\theta^{ss}}{B}) e^{\theta^{ss}} & -1 - Da \, e^{\theta^{ss}} \end{pmatrix}, \quad (9)$$

and the corresponding two eigenvalues of the considered dynamical systems are:

$$\begin{pmatrix} \lambda_1 & 0 \\ 0 & \lambda_2 \end{pmatrix} = \begin{pmatrix} -1.0 & 0 \\ 0 & -1 + (B - 1 - \theta^{ss}) Da \, e^{\theta^{ss}} \end{pmatrix} \quad (10)$$

Both eigenvalues are real, and at least one eigenvalue is a negative constant ($\lambda_1 = -1.0$). The second eigenvalue (λ_2) determines the stability of the whole system:

- $\lambda_2 < 0$: the steady-state along the manifold is asymptotically stable, meaning perturbations will decay over time [1, 7]. The range to ensure $\lambda_2 < 0$ can be analytically determined as:

$$\mathbf{I}_1 = \{\theta^{ss} : 0 < \theta^{ss} < \theta_{\text{Ext}}^{\text{ss}}\} \quad \text{or} \quad \mathbf{I}_2 = \{\theta^{ss} : \theta^{ss} > \theta_{\text{Ign}}^{\text{ss}}\} \quad (11)$$

with

$$\theta_{\text{Ext}}^{\text{ss}} = B - 1 + W_{-1} \left(-\frac{e^{1-B}}{Da} \right), \quad \text{and} \quad \theta_{\text{Ign}}^{\text{ss}} = B - 1 + W_0 \left(-\frac{e^{1-B}}{Da} \right).$$

Here W_0 and W_{-1} are two branches of Lambert W function [6]. We notice that to get a negative eigenvalue, there are two regimes, where stable steady-state solutions are obtained: If θ^{ss} falls within \mathbf{I}_1 , the system reaches one stable regime describing a failed spark ignition solution; If θ^{ss} falls within \mathbf{I}_2 , the system reaches the other stable regime where successful spark ignition is achieved.

- $\lambda_2 > 0$: the steady-state becomes unstable and behaves like a saddle point [1, 7]. The corresponding range for a positive λ_2 reads

$$\mathbf{I}_3 = \{\theta^{ss} : \theta_{\text{Ext}}^{\text{ss}} < \theta^{ss} < \theta_{\text{Ign}}^{\text{ss}}\}.$$

Figure 2 shows the dependence of $\theta_{\text{Ext}}^{\text{ss}}$ and $\theta_{\text{Ign}}^{\text{ss}}$ on dimensionless heat release B (left) and on Damköhler number (right). The left subfigure in Fig. 2 indicates that $\theta_{\text{Ign}}^{\text{ss}}$ changes only slightly with the Damköhler number, while $\theta_{\text{Ext}}^{\text{ss}}$ increases with Da^{-1} values. This means that with a smaller Damköhler number (larger Da^{-1} value, shorter residence time or longer chemical reaction time-scale), the stable \mathbf{I}_1 regime becomes wider, and the system is more likely to encounter a failed ignition solution.

The right subfigure in Fig. 2 shows an interesting phenomenon. At small values of dimensionless heat release (in this figure, when B is less than approximately 5.5), the unstable regime \mathbf{I}_3 does not exist. As the B -value increases, the unstable regime widens. Even more noticeably, for large values of B , the stable extinction regime \mathbf{I}_1 narrows, with $\theta_{\text{Ext}}^{\text{ss}}$ approaching zero. Physically, this indicates that with very high reaction heat release, the system is far less likely to experience failed spark ignition and is more likely to be successfully ignited.

4 Conclusions

The classic Perfectly Stirred Reactor (PSR) model is extended by introducing an additional energy source to simulate the spark ignition process in a laminar premixed flame in a counterflow configuration. A non-dimensional governing ODE system is formulated for both temperature and

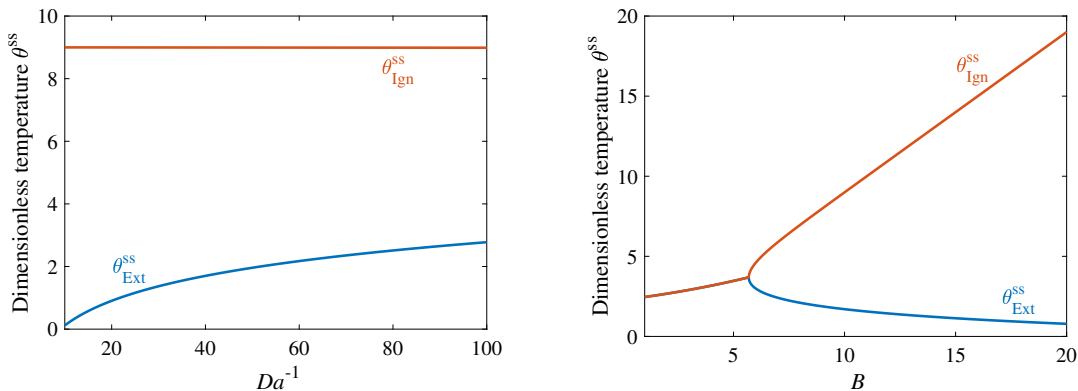


Figure 2: Dependence of $\theta_{\text{Ext}}^{\text{ss}}$ and $\theta_{\text{Ign}}^{\text{ss}}$ on dimensionless heat release B (left) and on Damköhler number (right). Left: $B = 10$, right: $Da^{-1} = 40$. Other dimensionless variables are $\tau_s = 0.1$, $\beta = 40$. Source: from the authors.

fuel mass fraction, which depends on three key dimensionless variables: dimensionless heat release, dimensionless activation energy, and the Damköhler number.

The ODE system is analyzed mathematically and, based on the eigenvalue analysis, it is found that the equilibrium steady states exhibit two stable regimes: one corresponding to failed ignition and the other to successful ignition. The failed ignition regime becomes wider as the Damköhler number decreases and narrower with higher heat release from the chemical reaction. Further investigation by directly integrating the non-dimensional ODE system is being carried out to understand the impact of the Damköhler number, spark duration time, and dimensionless heat release on the ignition process.

References

- [1] N. P. Bhatia and G. P. Szegö. **Dynamical systems: stability theory and applications**. Vol. 35. Springer, 2006.
- [2] J. D. Buckmaster. **The mathematics of combustion**. SIAM, 1985.
- [3] D. A. Eichenberger and W. L. Roberts. “Effect of unsteady stretch on spark-ignited flame kernel survival”. In: **Combustion and Flame** 118.3 (1999), pp. 469–478.
- [4] A. Frendi and M. Sibulkin. “Dependence of minimum ignition energy on ignition parameters”. In: **Combustion Science and Technology** 73.1-3 (1990), pp. 395–413.
- [5] K. W. Jenkins, M. Klein, N. Chakraborty, and R. S. Cant. “Effects of strain rate and curvature on the propagation of a spherical flame kernel in the thin-reaction-zones regime”. In: **Combustion and Flame** 145.1-2 (2006), pp. 415–434.
- [6] J. Lehtonen. “The Lambert W function in ecological and evolutionary models”. In: **Methods in Ecology and Evolution** 7.9 (2016), pp. 1110–1118.
- [7] H. Leipholz. **Stability theory: An introduction to the stability of dynamic systems and rigid bodies**. Springer-Verlag, 2013.
- [8] U. Maas and J. Warnatz. “Ignition processes in hydrogen oxygen mixtures”. In: **Combustion and flame** 74.1 (1988), pp. 53–69.

- [9] E. F. Tarrazo, R. G. Miguel, and M. Sánchez. "Minimum ignition energy of hydrogen–ammonia blends in air". In: **Fuel** 337 (2023), p. 127128.
- [10] S. R. Turns. **Introduction to combustion**. Vol. 287. McGraw-Hill Companies New York, NY, USA, 1996.
- [11] C. Yu, S. Eckart, S. Essmann, D. Markus, A. Valera-Medina, R. Schießl, B. Shu, H. Krause, and U. Maas. "Investigation of spark ignition processes of laminar strained premixed stoichiometric NH₃-H₂-air flames". In: **Journal of Loss Prevention in the Process Industries** 83 (2023), p. 105043.
- [12] C. Yu, D. Markus, R. Schießl, and U. Maas. "Numerical study on spark ignition of laminar lean premixed methane-air flames in counterflow configuration". In: **Combustion Science and Technology** 195.9 (2023), pp. 2085–2109.
- [13] I. B. Zeldovich. "Mathematical theory of combustion and explosions". In: **Consultants Bureau** (1985).